Philipps Universität Marburg

High-Performance Computing of Hydrodynamic Dispersion in Cylindrical Packed Beds of Different Aspect Ratios

Siarhei Khirevich, Alexandra Höltzel, and Ulrich Tallarek

Department of Chemistry, Philipps-Universität Marburg, Hans-Meerwein-Strasse, 35032 Marburg, Germany

E-mail: khirevich@gmail.com, tallarek@staff.uni-marburg.de

Introduction

Random packings of spherical particles confined in a cylindrical conduit are a good model for particle-based chromatographic columns. A fundamental property of confined particulate packings is the geometrical wall effect, which originates in the impossibility to pack spherical particles tightly against a hard, flat column wall. This results in porosity (void space fraction) oscillations across the column cross-section, which persists over a length of several particle diameters from the column wall. For a mobile phase percolating through the packing, the porosity oscillations translate to a maldistribution of the flow velocity, which increases hydrodynamic dispersion and decreases the separation efficiency of the column. The amplitude and length of the porosity oscillations depend on various factors, such as the column diameter, the average bed porosity of the packing, the average particle size, and the particle size distribution.

Computer simulations allow a systematic study of the influence of these parameters on the resulting hydrodynamic dispersion in the packing. We employed a combination of advanced numerical techniques and high-performance computing systems (supercomputers) to perform three-dimensional pore-scale simulations of hydrodynamic dispersion in cylindrically confined monodisperse random sphere packings. Such packings were generated under a systematic variation of the column diameter, the bed porosity, and the degree of heterogeneity in the packing microstructure. The time evolution of the dispersion coefficient was monitored up to the asymptotic limit. Simulations were carried out over a broad range of reduced velocities, $0.05 \leq \nu \leq 500$, to observe diffusion-dominated, transient, and advection-dominated mass transport regimes.

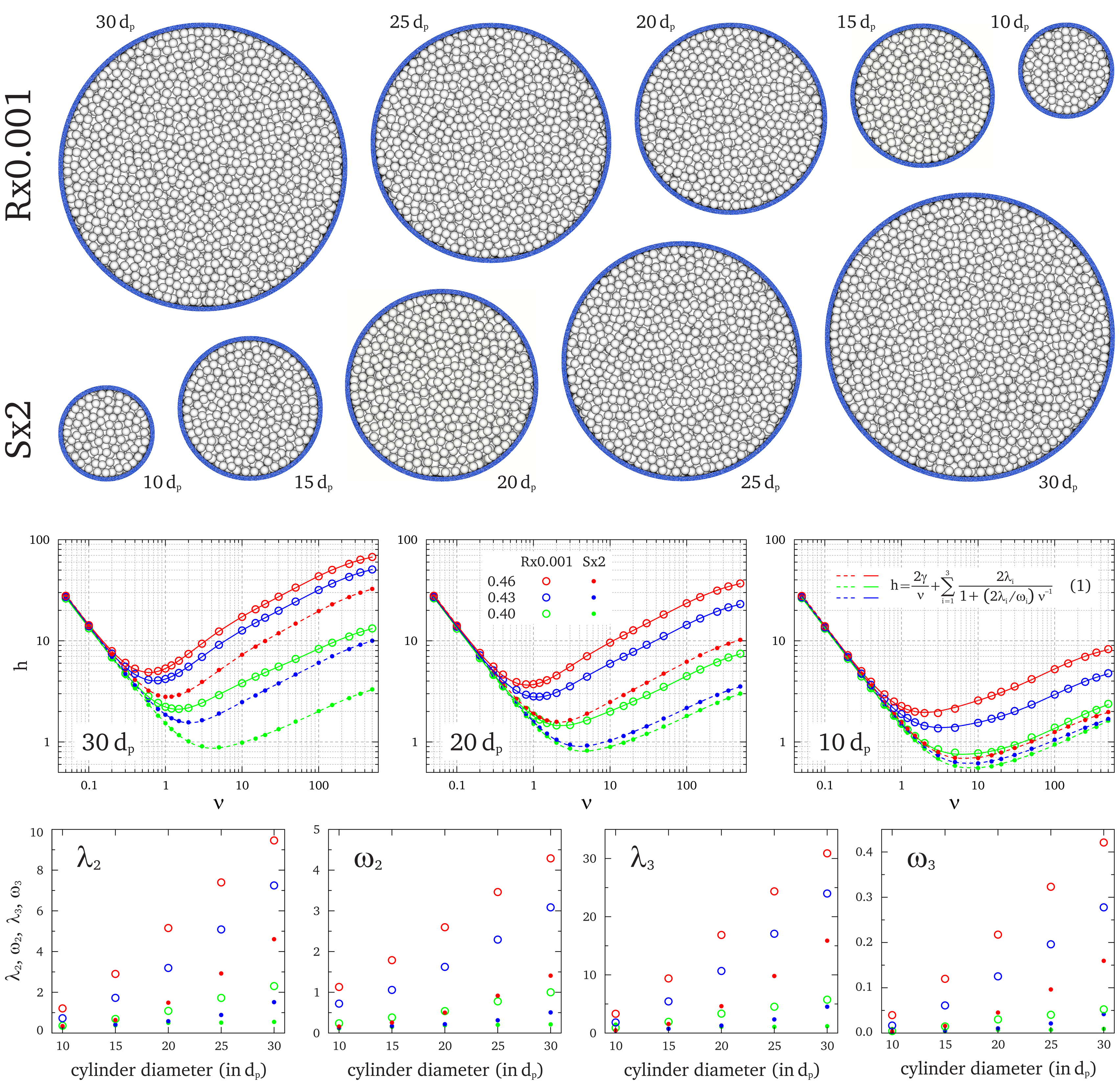

Figure 1. Top row: front view on the confined sphere packings of Rx0.001 and Sx2 types generated in cylindrical containers with cylinder-to-particle diameter ratio of 10, 15, 20, 25, and 30 at porosity of 0.43. **Middle row:** reduced plate height $h_L = H_L/d_p$ vs reduced velocity $\nu = u_{av} d_p / D_m$, where H_L is the height equivalent to a theoretical plate, d_p the sphere diameter, u_{av} the average mobile phase velocity, and D_m is the solute diffusivity in the mobile phase. Each data point represents the average of three generated packings. Solid lines are the best fits of the generalized Giddings equation[6] (1) to the reduced plate height data. The first term on the right hand side in equation (1) accounts for the effect of molecular diffusion while the second term describes eddy dispersion as the sum of three contributions — transchannel, short-range interchannel, and transcolumn (λ_i and ω_i are universal structural parameters characteristic of each contribution). The value of the obstruction factor γ in equation (1) was determined by monitoring the long-time limit of the time-dependent diffusion coefficient, while the values of λ_1 and ω_1 (transchannel contribution) were obtained from the periodic (unconfined) packings of the same porosity and packing type as their confined counterparts. **Bottom row:** Dependence of the parameters for the short-range interchannel (λ_2 and ω_2) and transcolumn (λ_3 and ω_3) contributions on packing protocol, cylinder diameter, and porosity. Values were obtained from the best fits of the comprehensive dataset of the middle row figures to equation (1).

Simulation details

Confined random packings of monosized hard spheres were generated in cylindrical containers using a modified Jodrey–Tory (JT) algorithm.[1,2] Generated packings have dimensions (denoted as "cylinder diameter" × "cylinder length") of $10d_p \times 1638d_p$, $15d_p \times 3072d_p$, $20d_p \times 6553.6d_p$, $25d_p \times 9830d_p$, and $30d_p \times 9830d_p$, which are sufficient for performing both statistical analysis of the packing microstructure and simulation of the hydrodynamic dispersion within the void space of a packing. The packings have porosities (void space fraction) of 0.40, 0.43, and 0.46. JT algorithm distributes randomly particle centers in the simulation domain and iteratively removes overlaps between spheres by spreading apart of two closest sphere centers on each iteration. Amount of spheres in the packing defines the final packing porosity, while variation of the initial sphere center positions and the magnitude of an individual displacement of the closest sphere pair on each JT iteration enables generation of the sphere packings with different microstructure. In other words, JT allows us to vary packing preparation protocol (or "packing type"), which results in the generation of more or less heterogeneous packings (referred to as "Rx0.001" and "Sx2", respectively) also in the case of fixed packing dimensions and porosity.

Pore-scale simulations of fluid flow in the void space of the generated packings were done using the lattice Boltzmann method (LBM), and simulations of the transport of inert tracers were performed with the Random Walk Particle Tracking method (RWPT). Both LBM and RWPT are well suited for parallel computing, and allowed us to perform efficient high-performance simulations on one of the world's fastest supercomputing system JUGENE (Jülich, Germany): the largest simulations for the packings with spatial dimensions of $30d_p \times 9830d_p$ were performed on 98 304 processor cores, and required about 50TB of system memory.

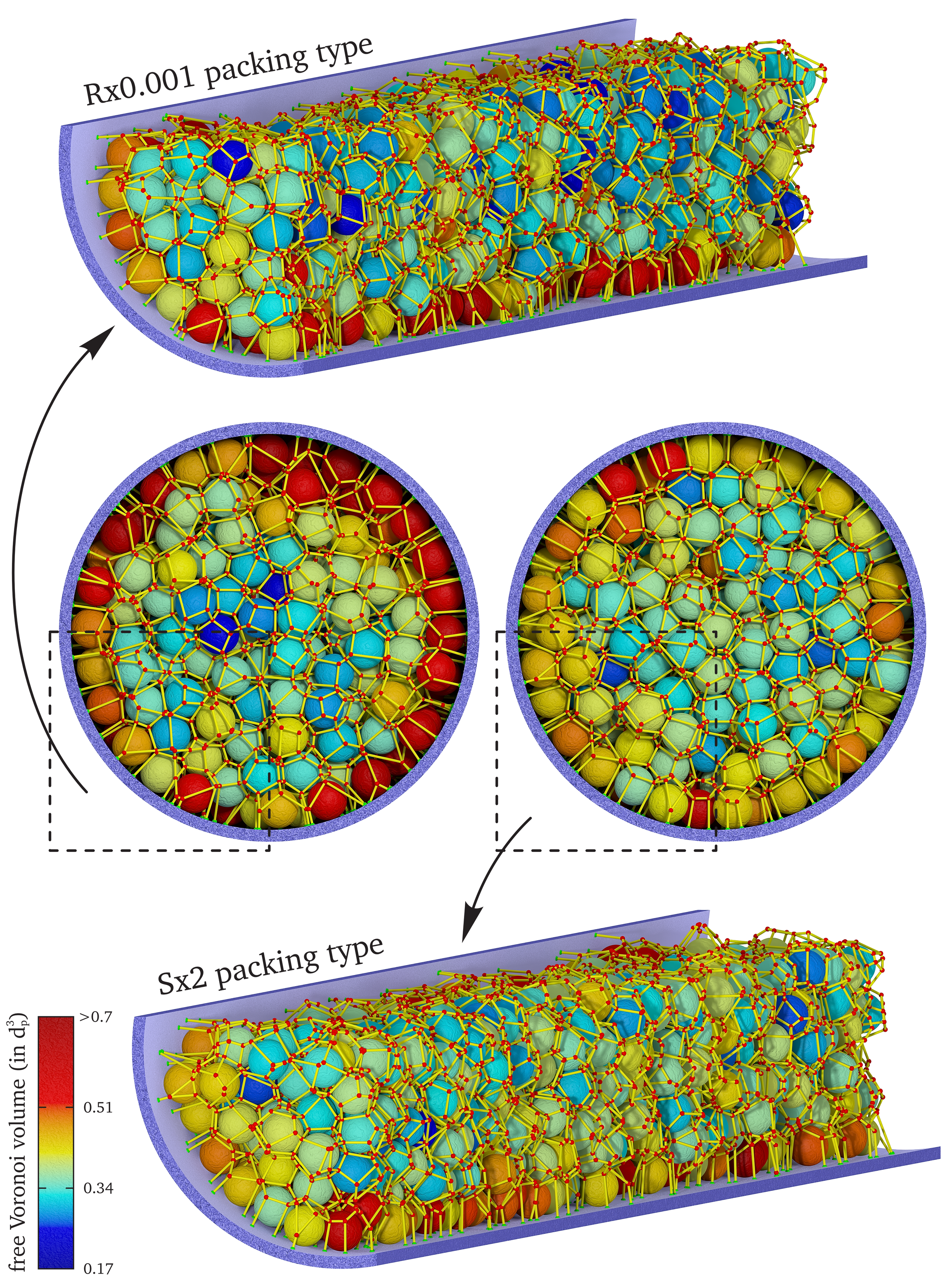

Figure 3. Tessellation of the confined Rx0.001 and Sx2 packings (with porosity of 0.43, generated in cylindrical containers with diameter of 10 d_p) into the Voronoi cells.[3,4] A Voronoi cell is the generalization of a Wigner–Seitz cell for disordered structures. For a packing of monosized spheres (or disks in 2D) it is

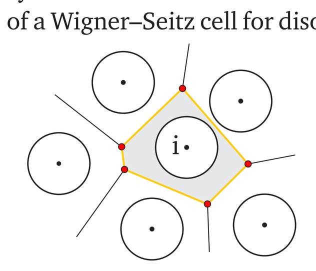

the polyhedron (polygon in 2D) that contains all points closer to a given sphere center (disk center in 2D) than to any other. A two-dimensional Voronoi cell of disk "i" is illustrated in the caption figure by the yellow polygon. Red nodes and yellow ridges are points located on equal distance from four (three in 2D) and three (two in 2D) spheres, respectively. Green nodes indicate locations where yellow ridges were truncated by the confining wall of the cylinder. Voronoi cell can be quantified by its volume, and a difference between the Voronoi volume of the cell and volume of the sphere located in this cell is termed as "free Voronoi volume" (or free Voronoi area in 2D). Gray region of the yellow polygon shown in the caption figure illustrates free Voronoi area of disk "i."

Porosity distributions

A well-known approach to estimate heterogeneity of a confined random sphere packing is to analyze the lateral porosity distribution of the packing. In the confined packings porosity distributions show damped oscillations in the near-wall region, resulting from the inability of the spheres to form a close packing against the flat wall. As can be seen in Figure 2, porosity oscillations with higher amplitude are observed for *more homogeneous* (at least, according to the packing preparation protocol and corresponding plate height values) packings.

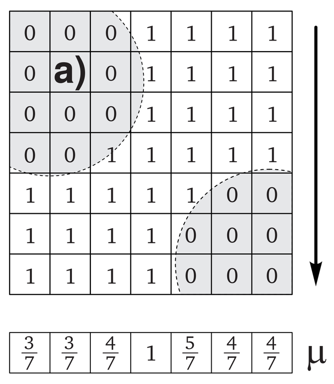

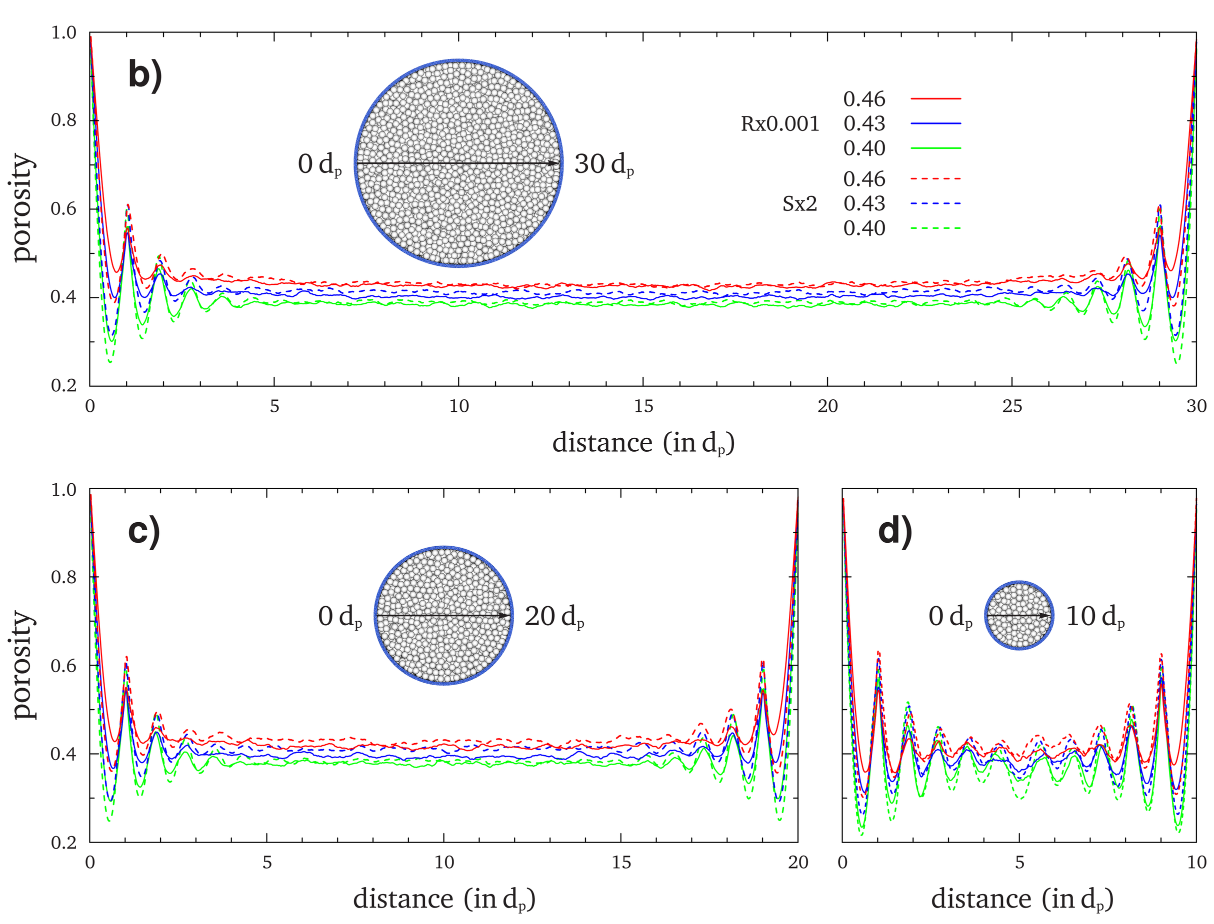

Figure 2. a) Schematic representation of the procedure used to determine lateral porosity distribution profiles in the generated sphere packings. The procedure included i) cover of the whole volume of the packing with the uniform cubic lattice; ii) each lattice voxel was assigned to "0" or "1" depending on the location of the voxel center, inside or outside the closest sphere, respectively; iii) calculation of the mean local porosity values by averaging amount of the fluid voxels as indicated by the arrow. **b, c, d)** Porosity distributions for the cylinders of Rx0.001 and Sx2 packing types with cylinder-to-particle diameter ratio of 30, 20, and 10, and porosity of 0.40, 0.43, and 0.46. Profiles were calculated along indicated arrows over the whole packing length.

Voronoi volume distributions

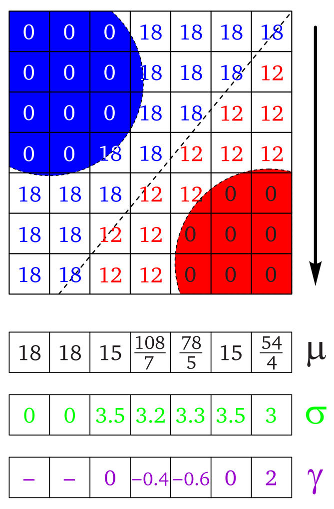

Figure 4. Top: Schematic representation of the procedure used to determine profiles of the statistical moments of the free Voronoi volume distribution. The procedure is similar to the one described in the caption of Figure 2, except that each lattice voxel is assigned to the value of free Voronoi volume of the closest sphere. **Right:** Slices of the distribution of free Voronoi volumes in the packings with porosity of 0.43 and cylinder-to-sphe-re diameter ratio of 10. The packings were generated using Rx0.001 and Sx2 packing protocols.

A sensitive analysis tool for probing the local packing density and disorder in packed beds is the determination of Voronoi cells, which contain all points closer to a given sphere center than to any other[3] (see more detailed explanation in the caption of Figure 3). Recently we have demonstrated that statistical moments (standard deviation and skewness) of the distribution of Voronoi volumes (volumes of Voronoi cells) are in good correlation with the plate height values in case of the periodic (unconfined) packings of different porosities and packing protocols. In this study we extend previously employed analysis to the case of confined packings. Figure 4 shows a schematic overview of the approach used to determine spatial distributions of the *free Voronoi volumes*. As can be seen in Figure 5, derived distributions reflect the difference in the simulated plate height values shown in the middle row of Figure 1.

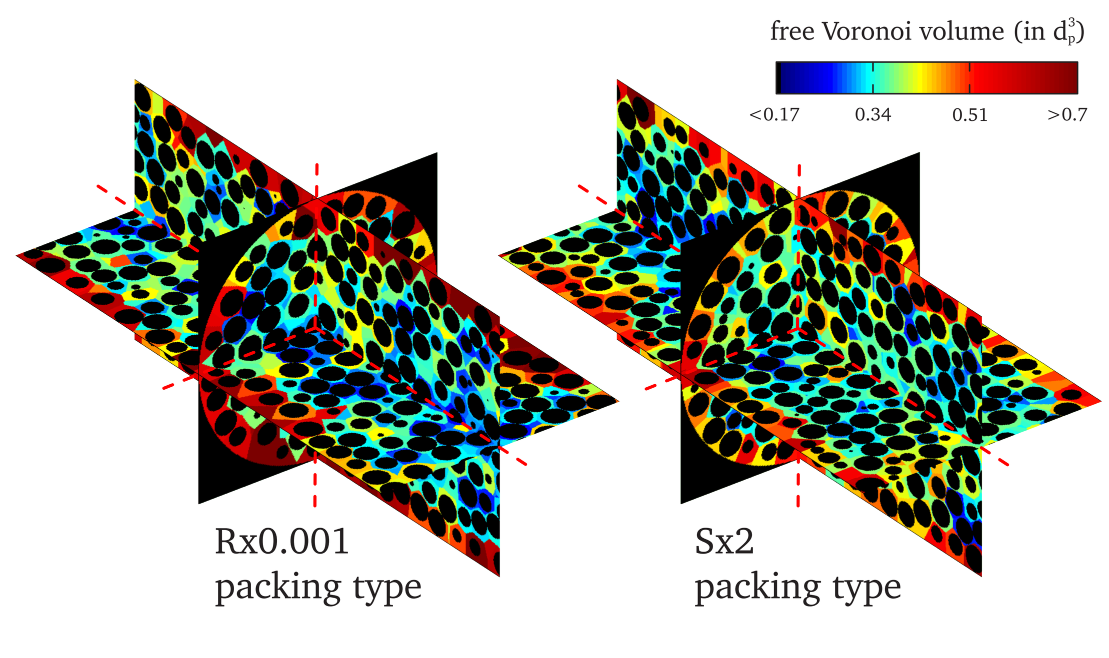

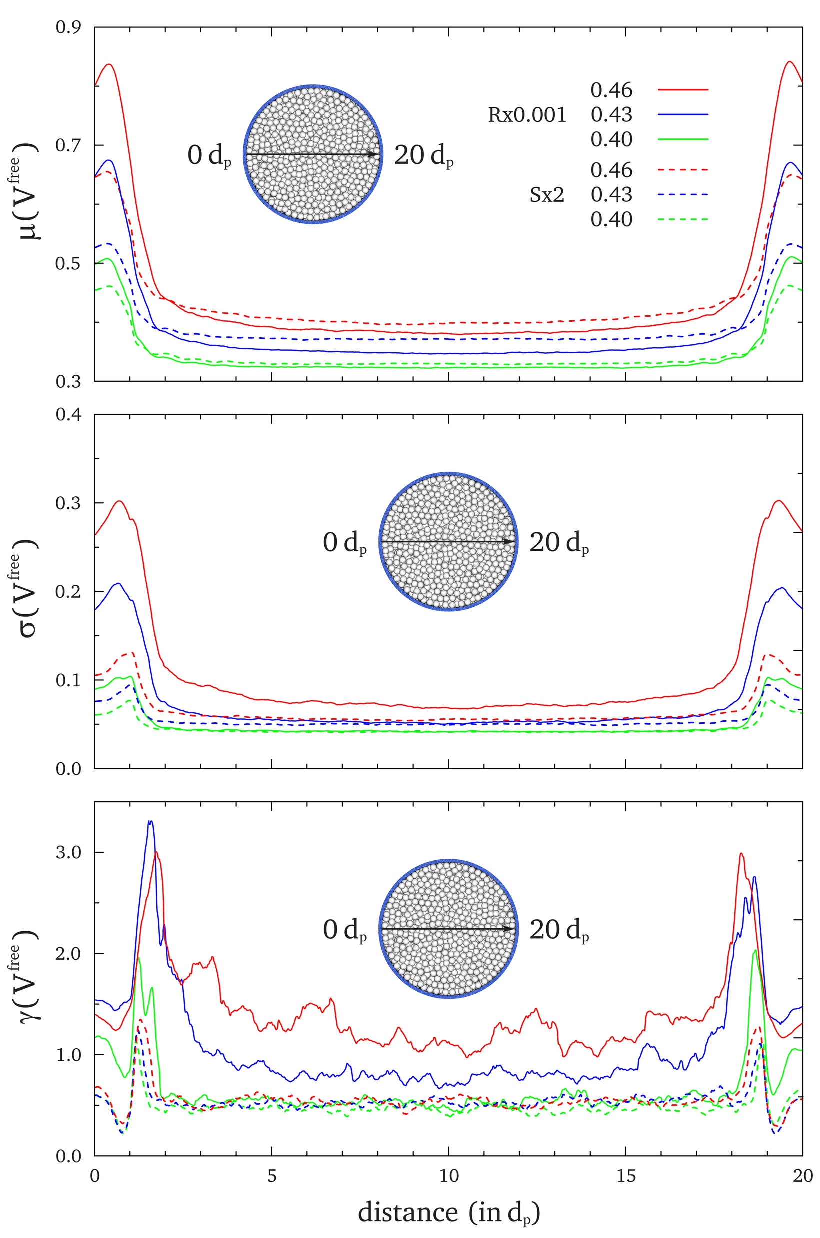

Figure 5. Profiles of average, standard deviation, and skewness of the free Voronoi volume distributions, calculated along indicated arrows over the whole packing length for the packings with porosities of 0.40, 0.43, and 0.46 generated using Rx0.001 and Sx2 packing protocols.

Conclusion

The presented simulation approach enabled i) generation of the random sphere packings with systematically varied geometrical parameters (diameter of the cylindrical packing container (d_c), porosity (ε), and the packing preparation protocol (Π)), and ii) high-resolution pore-scale simulations of transport (flow and hydrodynamic dispersion) in the void space of the generated packings. Carefully conducted transport simulations[5] resulted in an excellent fit of the generalized Giddings equation (1) to the simulated plate height data, resolving of the *individual* contributions of the dispersion term in (1), and demonstration of the systematic influence of d_c, ε, and Π on these contributions. In addition to the well-known fact of the influence of ε and d_c on the plate height values, it was shown a strong impact of the packing preparation protocol on h: the difference between the optimal plate height values of the packings with fixed d_c and ε but different Π can achieve three times. Geometry of the packing pore space was analyzed by i) "classical" approach based on the radial porosity distributions, and ii) a novel method based on the Voronoi volume distributions. Only the latter method demonstrated correlation between the geometrical descriptors and corresponding values of h.

Acknowledgments

Computational resources on IBM BlueGene/P platforms were provided by "Jugene" at FZJ (Forschungszentrum Jülich, Germany). We thank the DEISA Consortium (www.deisa.eu), co-funded through the EU FP6 project RI-031513 and the FP7 project RI-222919, for support within the DEISA Extreme Computing Initiative.

References

[1] Khirevich, S.; Daneyko, A.; Höltzel, A.; Seidel-Morgenstern, A.; Tallarek, U. *Statistical analysis of packed beds, the origin of short-range disorder, and its impact on eddy dispersion.* J. Chromatogr. A, 28: 4713, **2010**
[2] Jodrey, W. S.; Tory, E. M. *Computer simulation of close random packing of equal spheres.* Phys. Rev. A, 32: 2347, **1985**
[3] Okabe, A.; Boots, B.; Sugihara, K.; Chiu, S. N. *Spatial tessellations: concepts and applications of Voronoï diagrams.* John Wiley & Sons Ltd.: Chichester, England, **2000**
[4] Barber, C. B.; Dobkin, D. P.; Huhdanpaa, H. *The quickhull algorithm for convex hulls.* ACM Trans. Math. Softw., 22: 469, **1996**
[5] Khirevich, S.; Höltzel, A.; Seidel-Morgenstern, A.; Tallarek, U. *Time and length scales of eddy dispersion in chromatographic beds*. Anal. Chem., 81: 7057, **2009**
[6] Giddings, J. C. *Dynamics of Chromatography, Part 1: Principles and Theory*; Marcel Dekker: New York, **1965**